Peer Review File

Dynamically encircling an exceptional point through phase-tracked closed-loop control

Corresponding Author: Professor Xin Zhou

This file contains all reviewer reports in order by version, followed by all author rebuttals in order by version.

Version 0:

Reviewer comments:

Reviewer #1

(Remarks to the Author)
This study introduces a phase-locked loop (PLL) technique to the process of dynamical encircling of exceptional points (EPs) in non-Hermitian systems. In the conventional case of dynamically encircling EPs (mostly realized in waveguides system), non-adiabatic transitions cannot be avoided, resulting in the phenomenon of asymmetric mode switching. In the current work with the PLL technique, in contrast, the system dynamically binds excitation frequencies to response phases, ensuring smooth traversal of eigenstates along the Riemann surfaces and effectively avoiding non-adiabatic transitions. In this way, the topological structure of a non-Hermitian system around EPs can be measured since the evolution of eigenstates is adiabatic. In experiments, the authors designed an on-chip non-Hermitian MEMS resonator, where the structural asymmetry is employed to introduce a damping rate difference between two coupled modes. Through precise electrical control of parameters, the feasibility of EP encircling is validated, with experimental results showing agreement with theoretical predictions. This is overall an interesting work. It provides a new technique for probing the topology of non-Hermitian systems. I would be happy to support the publication of the work after the authors address my following comments.
1. While conventional static measurements can already characterize both the state exchange dynamics and Riemann surface topology near EPs, what distinct advantages does the proposed approach offer for such investigations compared to conventional static methods?
2. The experiment employed a rectangular path to dynamically encircle the EP, where only one parameter is varied at any time. Could alternative path geometries (e.g., circular paths) also be utilized such that the two system parameters vary simultaneously?
3. The PLL technique adjusts the excitation frequency in real-time via a feedback to synchronize the parameter variation rate with the system response, thereby emulating an adiabatic process. Is it possible to intentionally induce non-adiabatic transitions by modifying the PLL feedback parameters (e.g., reducing the PID controller’s response speed or altering the phase-locking conditions)? If so, the proposed platform can also be used to probe non-Hermitian physics with non-adiabatic transitions.
4. Some typos to be corrected:
In Line 12 of the caption of Fig. 3, “frequence (c)” should be revised to “frequency (d)”.
In Line 5 of the caption of Fig. 4, “(green curve)” should be corrected to “(purple curve)”.

Reviewer #2

(Remarks to the Author)
In the manuscript, the authors have presented a new method for smoothly traversing the eigenfrequency Riemann surface of non-Hermitian systems. By measuring the instantaneous phase-tracked hybrid state information, one can extract the Hamiltonian information and reconstruct the imaginary part of the eigenvalue and eigenstates. The idea is novel, and the presented results are quite solid. This is an interesting and timely work in the field of non-Hermitian photonics, and I in general support its publication, pending the authors address the following issues:
1. Since the presented work includes experimental demonstrations, it is better to include the device layout in the main text.
2. The fabricated 6-inch wafer contains 333 devices. Do all these devices have identical properties, such as resonances and damping rates?
3. What is the tuning range and speed of the fabricated microelectromechanical device?
4. What is the practical application of the proposed non-Hermitian system?

Reviewer #3

(Remarks to the Author)
This manuscript presents a novel experimental approach to dynamically encircle exceptional points (EPs) in non-Hermitian systems by leveraging a phase-locked loop (PLL) technique. The authors address a key challenge in the field—the difficulty of achieving continuous and controlled traversal along the Riemann surfaces of non-Hermitian eigenvalues due to non-adiabatic transitions. By coupling the excitation frequency of steady states to their response phases, the proposed method maintains resonance and enables robust, phase-tracked encircling of EPs. The technique is demonstrated within a fully electrically controlled microelectromechanical system, showcasing practical implementation and in-situ tunability. The paper is well written and this work provides a significant advance in the study of non-Hermitian topologies, particularly by offering a scalable and experimentally accessible route to probing Riemann surfaces dynamically. I believe the manuscript is promising, but I would appreciate some clarifications that could enhance its clarity and impact.

1) Although they mention that the encircling of the EP does not depend on the direction of encircling. Does it depend on the starting point? Whether the encircling starts in the PT-symmetric or PT-broken phase?

2) The manuscript focuses on the dynamical encircling of a single EP using the PLL-based approach. However, if the system contains two nearby EPs, how does the method extend to characterize or encircle both? Specifically, can the authors shed some light on: How does the PLL technique respond when the control loop passes near or around both EPs? Does the proximity of the two EPs influence the transport behavior—particularly the emergence or suppression of non-chiral dynamics when the system starts in the symmetry-broken phase? If the control loop encloses both EPs, does the resulting behavior depend solely on the starting point of the loop, or are there qualitatively new phenomena (e.g., interference between EPs or modified topology) that arise?

3) How do your findings relate to recent developments in non-Hermitian topology? Specifically, is the phase-tracked dynamical encircling connected to any topological invariants—such as spectral winding numbers—defined over the control parameter loop? Clarifying this connection would help in the broader context of non-Hermitian topological physics.

Version 1:

Reviewer comments:

Reviewer #1

(Remarks to the Author)
The authors have addressed all my concerns in a satisfactory way. I sincerely thank the authors for their efforts in improving their work. I recommend the publication of the work in its present form.

Reviewer #2

(Remarks to the Author)
The authors have made significant efforts in improving the manuscript. The revised manuscript can be accepted as is now.

Reviewer #3

(Remarks to the Author)
The authors have thoroughly addressed the previous concerns, and the refined version of the manuscript significantly improves the overall quality, clarity, and impact of the work. The revisions strengthen the presentation and resolve the issues raised in the earlier review. I find that the manuscript now meets the standards required for publication and can be recommended for publication in its current form.

Response to Reviewers

We express our sincere gratitude to the reviewers for their valuable reviews. The manuscript has been modified accordingly to address the feedback received. Please find below our response to the reviewers. Reviewers' comments are in **blue**, authors' responses are in **black**, and the **red** parts indicate the corresponding modifications in the manuscript.

Reviewer #1 (Remarks to the Author):

This study introduces a phase-locked loop (PLL) technique to the process of dynamical encircling of exceptional points (EPs) in non-Hermitian systems. In the conventional case of dynamically encircling EPs (mostly realized in waveguides system), non-adiabatic transitions cannot be avoided, resulting in the phenomenon of asymmetric mode switching. In the current work with the PLL technique, in contrast, the system dynamically binds excitation frequencies to response phases, ensuring smooth traversal of eigenstates along the Riemann surfaces and effectively avoiding non-adiabatic transitions. In this way, the topological structure of a non-Hermitian system around EPs can be measured since the evolution of eigenstates is adiabatic. In experiments, the authors designed an on-chip non-Hermitian MEMS resonator, where the structural asymmetry is employed to introduce a damping rate difference between two coupled modes. Through precise electrical control of parameters, the feasibility of EP encircling is validated, with experimental results showing agreement with theoretical predictions. This is overall an interesting work. It provides a new technique for probing the topology of non-Hermitian systems. I would be happy to support the publication of the work after the authors address my following comments.

1. While conventional static measurements can already characterize both the state exchange dynamics and Riemann surface topology near EPs, what distinct advantages does the proposed approach offer for such investigations compared to conventional static methods?

Response:

Thank you very much for your thoughtful and valuable comments. We greatly appreciate your insights and recognize that traditional static measurements play a crucial role in characterizing the topological properties of EP singularities. We agree that such studies are essential for deepening our understanding of the topological features of non-Hermitian singularities. However, we would like to highlight some practical limitations associated with static measurements.

Firstly, static measurements rely on a discrete sampling approach to gather information about the eigenvalues or eigenstates along the encircling path. While this method facilitates the observation of the topological characteristics of EPs, it inherently lacks the ability to represent genuine continuous encircling. For practical applications of non-Hermitian topological properties, continuous and dynamical encircling is critical. Our proposed method allows for a direct investigation of key topological properties, such as genuine eigenvalue braiding and real-time Berry phase accumulation.

Additionally, conventional static testing necessitates fitting the spectral response at each sampling point to extract the system's eigenvalues or eigenstates along the encircling path, which can lead to considerable computational redundancy. In contrast, our approach simplifies this process by requiring only the measurement of the amplitude, phase, and resonant frequency of the system during continuous dynamic encircling. By integrating these measurements with the intrinsic resonator parameters obtained beforehand, we can effectively construct the system's instantaneous Hamiltonian and reconstruct its eigenvalues or eigenstates, as elaborated in the **Discussion** section. This innovative method significantly reduces computational redundancy.

Changes made:

We have added a relevant discussion in the **Introduction** section as "However, the primary utility of discrete measurements resides in the characterization of topological properties within non-Hermitian systems, which inherently constrains the practical applications of topological properties. Notably, such measurements require spectral analysis at each discrete sampling point, introducing considerable computational redundancy. Dynamic measurements provide a methodology to mitigate the aforementioned challenges, while achieving genuine continuous braiding or real-time accumulation of the Berry phase through dynamic execution of smooth encircling remains a formidable challenge, especially since the dynamical encircling of EPs often encounters non-adiabatic transitions."

2. The experiment employed a rectangular path to dynamically encircle the EP, where only one parameter is varied at any time. Could alternative path geometries (e.g., circular paths) also be utilized such that the two system parameters vary simultaneously?

Response:

Thank you for pointing out the concern about the geometry encircling path. We sincerely apologize for the confusion caused due to the experimental design issues. In fact, the dynamically encircling scheme based on phase-tracked closed-loop control that we propose does not rely on the special design of the encircling trajectory. It depends on the unique mapping relationship between the excitation frequency ω_{d} and the phase response $\theta = -\mathrm{Arg}[\chi_1(\omega_{\mathrm{d}})]$. By using the PLL to lock the system to the resonant phase corresponding to its eigenfrequency (i.e., $\theta[\mathrm{Re}(\lambda_{\pm})]$), the excitation frequency can be locked to any point on the Riemann surface of the eigenfrequency to achieve stable oscillations. Therefore, by presetting the parameters of the phase-tracking module to accurately trace the phase evolution trajectory during EP encircling, we can achieve smooth encircling of EP along arbitrary geometric paths.

Changes made:

We have added a circular path in the revised text to demonstrate the feasibility of our proposed method under simultaneous variation of two parameters: the pump strength ($V_{\mathrm{p}}(t) = 0.3 + 0.2\cos(\frac{\pi}{30}t)(\mathrm{V})$) follows a cosinusoidal time dependence, while the pump frequency detuning ($\delta_{\mathrm{p}}(t) = 2\pi \cdot 0.2\sin(\frac{\pi}{30}t)(\mathrm{Hz})$) varies sinusoidally.

The results are shown in **Fig. R1**.

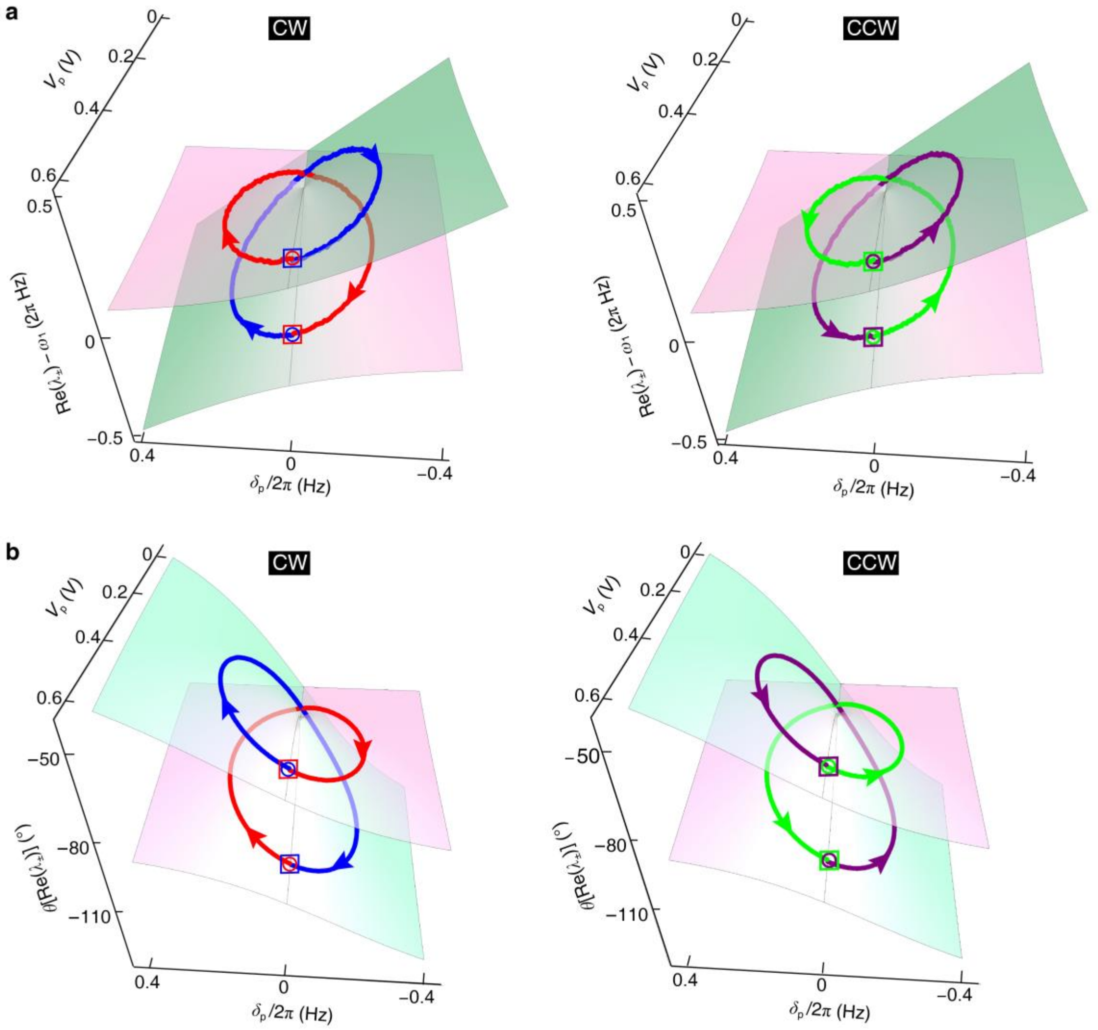

Fig. R1. Results of the smoothly encircling of EP with a circular trajectory. a, The phase-tracked closed-loop oscillation frequencies for the CW encircling process starting from the high-frequency sheet (red curve), the CW encircling process from the low-frequency sheet (blue curve), the CCW encircling process from the high-frequency sheet (purple curve), and the CCW encircling process from the low-frequency sheet (green curve) smoothly evolve on the $\mathrm{Re}[\lambda_\pm(t)]$ Riemann surface. The circles and squares denote the start/end points of the encircling trajectories on the high and low-frequency sheets, respectively. The arrow indicates the direction. **b**, The corresponding tracked phases for the four encircling processes. The colors on all the surfaces correspond to the imaginary part $\mathrm{Im}(\lambda_\pm)$ of the eigenvalues.

(1) From Line 1 to Line 4 on Page 13 in the revised main text, we have added a

demonstration about the circular path: "The rectangular path above varies only one parameter at any time. We also constructed a circular path where two parameters are varied simultaneously to better demonstrate the feasibility of smoothly encircling EP through phase-tracked closed-loop control (see Methods). The full results of encircling EP with a circular path are shown in Extended Data Fig. 5."

(2) In the revised Methods Section, we have added a new subsection titled "Smoothly encircling of EP with a circular trajectory" to describe in detail the parameter variation for the circular path and the analysis of the results. And the results are presented in "Extended Data Fig. 5".

3. The PLL technique adjusts the excitation frequency in real-time via a feedback to synchronize the parameter variation rate with the system response, thereby emulating an adiabatic process. Is it possible to intentionally induce non-adiabatic transitions by modifying the PLL feedback parameters (e.g., reducing the PID controller's response speed or altering the phase-locking conditions)? If so, the proposed platform can also be used to probe non-Hermitian physics with non-adiabatic transitions.

Response:

Thank you for pointing out this interesting issue. Indeed, it is possible to adjust the phase-locking conditions to achieve non-adiabatic transitions. As mentioned in the main text, the system has two eigenstates at a single parameter point of the encircling trajectory, with the high-frequency ($\mathrm{Re}(\lambda_+)$) and low-frequency ($\mathrm{Re}(\lambda_-)$) eigenstates corresponding to their respective resonant phases ($\theta\{\mathrm{Re}(\lambda_\pm)\} = -\mathrm{Arg}\{\chi_1[\mathrm{Re}(\lambda_\pm)]\}$). Therefore, we can achieve a transition of the oscillation frequency between the high-frequency sheet and the low-frequency sheet **by deliberately controlling the tracking phase $\boldsymbol{\theta}$ of the PLL to convert between $\boldsymbol{\theta}\{\mathbf{Re}(\boldsymbol{\lambda}_+)\}$ and $\boldsymbol{\theta}\{\mathbf{Re}(\boldsymbol{\lambda}_-)\}$.**

Changes made:

(1) In the revised main text, we have added a clarification in the "**Discussion**" section as "Beyond emulating adiabatic evolution, our proposed method can also induce non-

adiabatic transitions by intentionally modulating the resonant phase switch between high-frequency and low-frequency sheets (see Methods), providing a platform for exploring the non-Hermitian physical properties of non-adiabatic transitions."

(2) We have added a new part titled "Non-adiabatic transitions through phase-tracked closed-loop control" to demonstrate the details of inducing non-adiabatic transitions, and the experimental results are also shown in "Extended Data Fig. 6. Results of non-adiabatic transitions through phase-tracked closed-loop control", and **Fig. R2**.

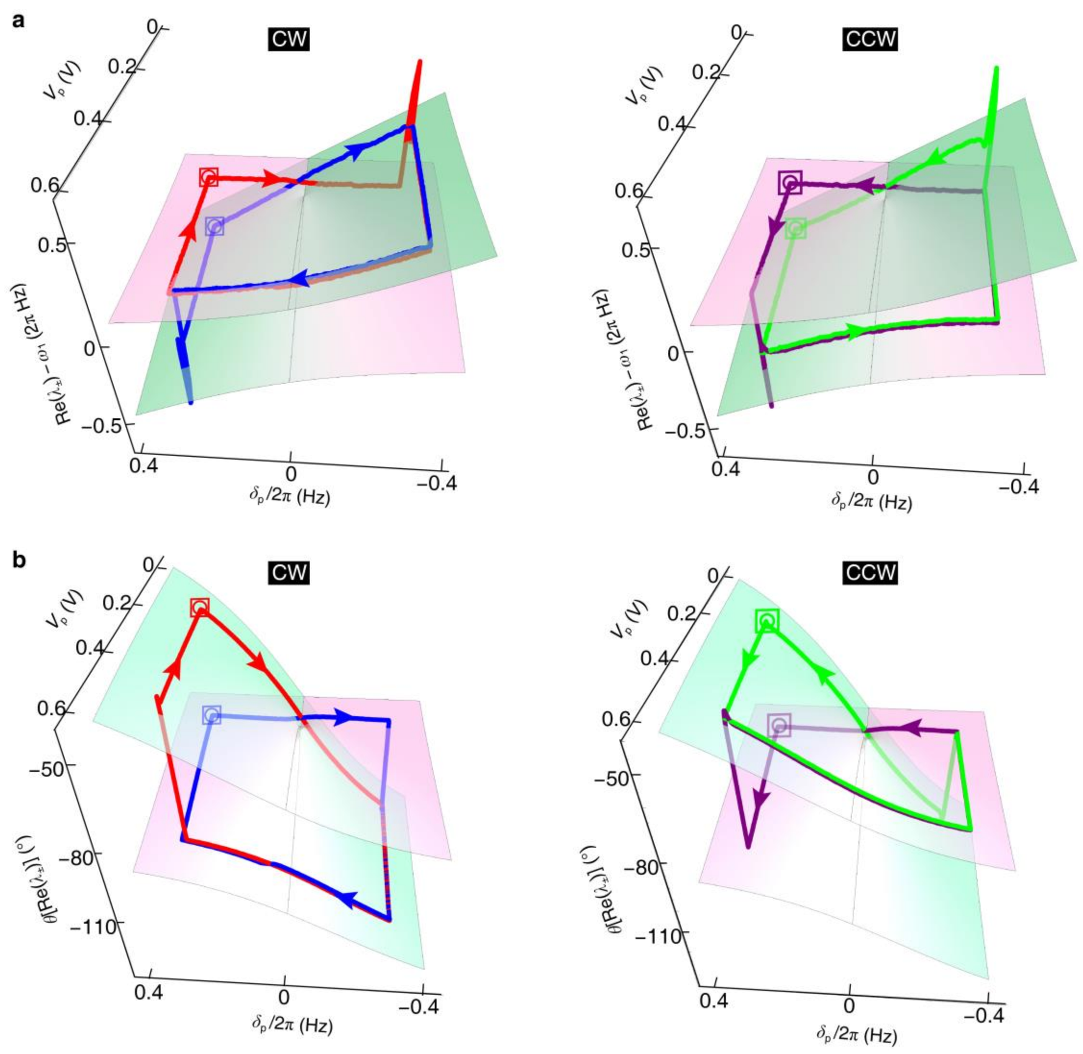

Fig. R2. Results of non-adiabatic transitions through phase-tracked closed-loop control. a, The phase-tracked closed-loop oscillation frequencies for the CW encircling process starting from the high-frequency sheet (red curve), the CW encircling process from the low-frequency sheet (blue curve), the CCW encircling process from the high-frequency sheet (purple curve), and the CCW encircling process from the low-frequency sheet (green curve) exhibit a transition between the high-and low-frequency sheets of the Riemann surface in lower-loss states. The circles and squares denote the start/end points of the encircling trajectories on the high and low-frequency sheets, respectively. The arrow indicates the direction. **b**, The corresponding tracked phases for the four encircling processes. The colors on all the surfaces represent the system's energy dissipation, with pink indicating low-loss states and cyan representing high-loss states.

4. Some typos to be corrected:

In Line 12 of the caption of Fig. 3, “frequence (c)” should be revised to “frequency (d)”.

In Line 5 of the caption of Fig. 4, “(green curve)” should be corrected to “(purple curve)”.

Response:

Thank you for the careful review and suggestions. We have corrected the misspellings and have checked the writing of the whole paper to avoid similar mistakes.

Changes made:

(1) In line 12 of the caption of Fig. 3, we have corrected the mistake to “and the corresponding oscillation frequency (**d**) of the encircling process”.

(2) In line 5 of the caption of Fig. 4, we have corrected the mistake to “the CCW encircling process from the high-frequency sheet (purple curve), and the CCW encircling process from the low-frequency sheet (green curve)”.

Reviewer #2 (Remarks to the Author):

In the manuscript, the authors have presented a new method for smoothly traversing the eigenfrequency Riemann surface of non-Hermitian systems. By measuring the instantaneous phase-tracked hybrid state information, one can extract the Hamiltonian information and reconstruct the imaginary part of the eigenvalue and eigenstates. The idea is novel, and the presented results are quite solid. This is an interesting and timely work in the field of non-Hermitian photonics, and I in general support its publication, pending the authors address the following issues:

1. Since the presented work includes experimental demonstrations, it is better to include the device layout in the main text.

Response:

We would like to express our sincere thanks to you for the valuable feedback, which is very constructive for revising the manuscript.

Indeed, the on-chip non-Hermitian device is constructed from a silicon MEMS disk resonator, which consists of multiple concentric rings connected by an intermediate anchor. The resonator is segmented into 12 fan-shaped sectors, with single-thick beams and double-thin beams arranged alternately between adjacent sectors to modulate the thermo-elastic damping of the n=3 (n is the wave number) mode and induce non-Hermitian properties, as shown in Extended Data Fig. 1. Additionally, we uniformly arranged 24 electrodes around the structure's surrounding to enable the excitation, detection, and tuning of the resonator.

Changes made:

We have added the 3D model diagram and the microscope image of the device to describe the device layout in revised Fig. 2a. The revised Fig. 2a is shown as **Fig. R3**.

a

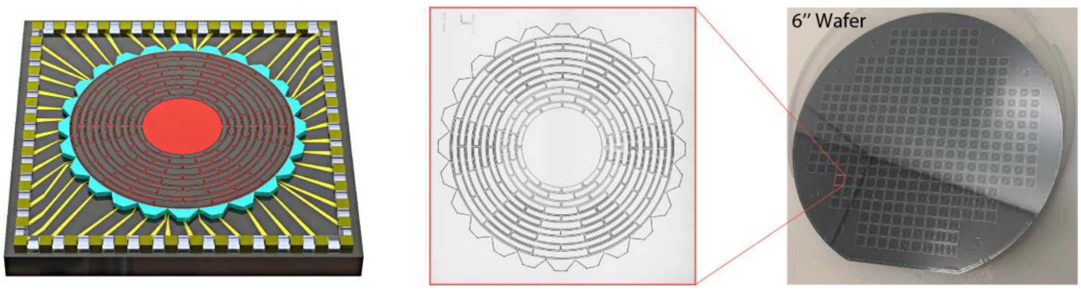

Fig. R3. The layout of this non-Hermitian resonator, where the left one shows the 3D model diagram, the right one shows a wafer containing 333 devices, and the middle one displays the microscope image of a single device.

2. The fabricated 6-inch wafer contains 333 devices. Do all these devices have identical

properties, such as resonances and damping rates?

Response:

We thank the referee for raising this point. Indeed, our resonators are fabricated via MEMS processes. Theoretically, resonators of identical design from the same fabrication batch possess nearly identical resonant frequencies and damping ratios. However, we implemented a gradient variation in beam thickness difference across these 333 devices, which produced **a gradient variation in frequency splitting** while maintaining nearly identical damping ratios.

In the initial idea, we considered utilizing ordinary coherent coupling to regulate the coupling strength of the non-Hermitian MEMS resonator, which requires the resonator to have two near-degenerate modes with matched natural frequencies. However, to satisfy the damping mismatch required for the non-Hermitian resonator, we implemented a special design for the beams at the nodal positions of the resonator's n=3 modes. Specifically, the structure features an alternating arrangement of double-thin beams and single-thick beams, as shown in "**Device design**" and "**Extended Fig. 1**". This specialized design may introduce increased fabrication errors of the beams, thereby affecting the resonator's stiffness and inducing significant frequency splitting between the two operational modes. Therefore, based on the ideal structural parameters of the frequency-matched resonator, we implemented a gradient-based design for the thickness variation of the resonator's beams. The frequency splitting of these resonators shows a gradient change, and the damping ratios are nearly identical, as shown in the **Table. R1**. Consequently, there must be some prototypes in these devices that satisfy the condition of frequency matching, thereby enabling the construction of EPs through ordinary coherent coupling.

In previous studies, dynamic coupling has been applied to the regulation of coupling between frequency-mismatched modes [e.g., Okamoto, Hajime, et al. "Coherent phonon manipulation in coupled mechanical resonators." Nature Physics 9.8 (2013): 480-484.]. Thus, we employ **Device # -40**, exhibiting the highest dissipation difference, as our experimental platform in this study. Using dynamic coupling, we successfully observe the Riemann surface of eigenvalues, as shown in **Fig. 2c** in the main text. The non-Hermitian system constructed by dynamic coupling forms the research platform of the continuous dynamic encircling of EPs applied in this paper.

Table. R1. Properties of the designed non-Hermitian MEMS resonators

#	f_1 (Hz)	f_2 (Hz)	Δf (Hz)	γ_1 (2πHz)	γ_2 (2πHz)	$\Delta\gamma$(2πHz)
-40	51161.483	50651.584	-509.899	0.91732	0.67726	0.24006
-30	50025.678	49619.113	-406.565	0.87208	0.64305	0.22903
-20	48626.976	48206.200	-420.776	0.78209	0.61450	0.16759
-16	49016.899	48945.584	-71.315	0.78209	0.60515	0.17694
-10	49468.787	49815.246	346.459	0.84657	0.66872	0.17785

As can be seen in the Table. R1, **Device # -16** exhibits the smallest frequency splitting, measuring -71.315 Hz. Through electrostatic tuning, we can adjust the two modes to a frequency-matched state. Following our initial idea, we also conducted investigations using **Device # -16**. By employing electrostatic negative-stiffness perturbations to precisely tune both the system's frequency degeneracy and coupling strength, we successfully observed the Riemann surface of complex eigenvalues, as shown in **Fig. R4**, those results will be presented in our ongoing future work. In our follow-up, next work, we will use Device # -16 as the platform to study topological properties in non-Hermitian systems, including eigenvalue braiding and Berry phase using the dynamical encircling method proposed in this study.

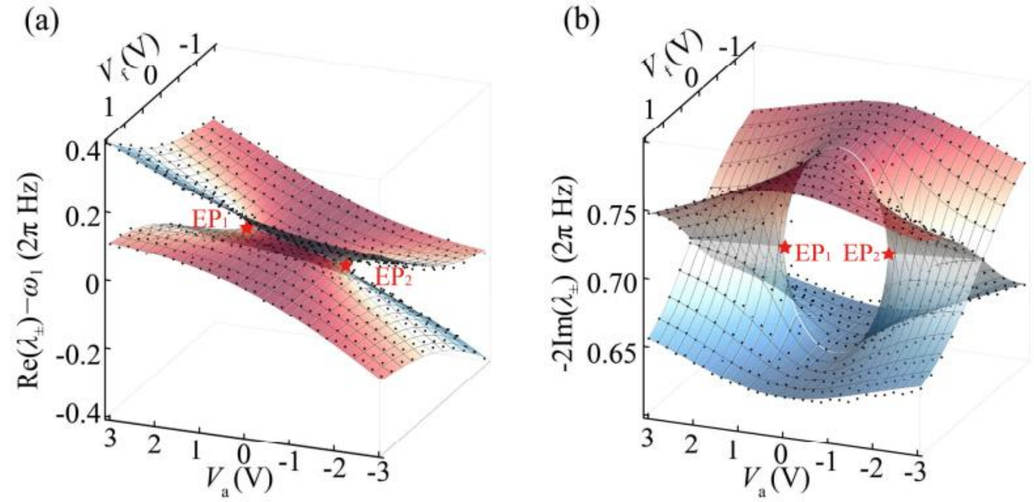

Fig. R4. Experimental results of eigenvalue Riemann surface for ordinary coherently coupled systems. (a) The resonant frequency and (b) The linewidth of the non-Hermitian system. The red stars mark two exceptional points.

3. What is the tuning range and speed of the fabricated microelectromechanical device?

Response:

Thank you for pointing out this interesting question. First, the non-Hermitian resonator we proposed is a fully electrically controlled MEMS resonator, which enables **in-situ** frequency modulation through electrostatic tuning. By applying a frequency-tuning voltage V_t to the electrodes along the vibrational axis of the resonator, electrostatic negative stiffness Δ_t can be generated in the resonator, which is expressed as

$$\Delta_t = \frac{A\epsilon_0 V_t(2V_0 - V_t)}{d_0^3 m_{eff}}$$

where A is the electrode area, d_0 represents the capacitive gap, ϵ_0 denotes the vacuum permittivity, V_0 is the bias voltage applied to the resonant structure, and m_{eff} stands for the effective mass. The resonant frequency after applying Δ_t becomes:

$$\omega_1 = \sqrt{\omega_0^2 + \Delta_t}$$

To prevent device breakdown due to high voltage, the potential difference threshold between the structure and electrodes is set to 60 V, with a fundamental frequency tuning capability of **100 Hz**. If the frequency splitting exceeds this range, dynamic coupling can be employed instead to compensate for the large frequency mismatch.

Furthermore, the frequency and coupling strength of this resonator employs an **in-situ regulation** method based on electrostatic negative stiffness, whose system stiffness matrix can be expressed as:

$$M = \begin{bmatrix} \omega_0^2 + \Delta_p/2 + \Delta_t & \Delta_p/2 \\ \Delta_p/2 & \omega_0^2 + \Delta_p/2 \end{bmatrix}$$

where Δ_t represents the electrostatic negative stiffness induced by the frequency-tuning voltage V_t as previously mentioned, while Δ_p denotes the electrostatic negative stiffness generated by the coupling-tuning voltage V_p. Consequently, **real-time regulation** of both frequency and coupling strength can be achieved by adjusting V_t and V_p.

Changes made:

From Line 2 to Line 3 on Page 7, we have made a statement about the tuning speed in the revised text as "The dynamic coupling can be regulated in real time by tuning the pump $V_p \cos(\omega_p t)$, showcasing remarkable in-situ controllability."

4. What is the practical application of the proposed non-Hermitian system?

Response:

We sincerely appreciate your evaluation and comment. This issue provides significant guidance for applied research on non-Hermitian MEMS resonators.

The primary research objective of this paper is the continuous, dynamically encircling of EPs, which is of importance for investigating the topological properties in non-Hermitian systems. Due to the presence of non-adiabatic transitions, the continuity of dynamically encircling an EP will be disrupted. Therefore, current research methodologies for investigating topological properties in non-Hermitian systems are predominantly limited to quasi-static discrete measurements. In this work, we demonstrate continuous, dynamical encircling of an EP through phase-tracked closed-loop control in our presented non-Hermitian system. Therefore, the proposed non-Hermitian system can be used as **a testbed for fundamental investigations of topological phenomena, including Berry phase accumulation and eigenvalue braiding.**

In addition, as a fully electrically controllable MEMS resonator, the proposed non-Hermitian resonator has the advantages of small size, low cost, and low power consumption, and has broad application prospects in **integrated sensing**. The non-Hermitian resonator is optimized based on a Hermitian disk MEMS gyroscope. Therefore, the resonator can also be used as a MEMS gyroscope to measure angular velocity. Furthermore, in several previous works [e.g., Lai, Yu-Hung, et al. "Observation of the exceptional-point-enhanced Sagnac effect." Nature 576.7785 (2019): 65-69.; Hokmabadi, Mohammad P., et al. "Non-Hermitian ring laser gyroscopes with enhanced Sagnac sensitivity." Nature 576.7785 (2019): 70-74.], the EPs in the non-Hermitian system have been applied to the sensitivity enhancement of the optical gyroscope, which inspires **enhancing the sensitivity of MEMS gyroscopes by using EPs**. If the Coriolis effect of the MEMS gyroscope can be enhanced by using EPs, the sensitivity of the MEMS gyroscope will be improved by orders of magnitude. The proposed non-Hermitian MEMS resonator provides a feasible platform for the study of **improving the performance of MEMS gyroscopes by using EP-enhanced sensing**, which is the goal of one of our future works.

Reviewer #3 (Remarks to the Author):

This manuscript presents a novel experimental approach to dynamically encircle exceptional points (EPs) in non-Hermitian systems by leveraging a phase-locked loop (PLL) technique. The authors address a key challenge in the field—the difficulty of achieving continuous and controlled traversal along the Riemann surfaces of non-Hermitian eigenvalues due to non-adiabatic transitions. By coupling the excitation frequency of steady states to their response phases, the proposed method maintains resonance and enables robust, phase-tracked encircling of EPs. The technique is demonstrated within a fully electrically controlled microelectromechanical system, showcasing practical implementation and in-situ tunability. The paper is well written and this work provides a significant advance in the study of non-Hermitian topologies, particularly by offering a scalable and experimentally accessible route to probing Riemann surfaces dynamically. I believe the manuscript is promising, but I would appreciate some clarifications that could enhance its clarity and impact.

1) Although they mention that the encircling of the EP does not depend on the direction of encircling. Does it depend on the starting point? Whether the encircling starts in the PT-symmetric or PT-broken phase?

Response:

Thank you very much for pointing out this vagueness. We are really sorry for the unclear presentation of the starting point of encircling in the previous manuscript. Indeed, our proposed dynamically encircling scheme is independent of the initial position where the parameter loop begins.

In the initial manuscript, we take $(V_{\mathrm{p}}, \delta_{\mathrm{p}}/2\pi) = (0.5\ \mathrm{V}, 0.3\ \mathrm{Hz})$ **in the PT-symmetric phase** as the base point and conduct four sets of encircling starting from the high-frequency sheet (lower-loss mode) and the low-frequency sheet (higher-loss mode), respectively. As illustrated in **Fig. 4**, the results show that phase-tracked closed-loop control effectively suppresses non-adiabatic transitions when the system starts from the PT-symmetric phase, regardless of the initial dissipation state.

And in the revised manuscript, we have added four sets of encircling starting from $(V_{\mathrm{p}}, \delta_{\mathrm{p}}/2\pi) = (0.1\ \mathrm{V}, 0.3\ \mathrm{Hz})$, **which is located in the PT-broken phase**. The starting points are located in the high and low-frequency sheets, respectively. In the CW encircling path, the control parameters vary linearly by the sequence: $[(V_{\mathrm{p}}, \delta_{\mathrm{p}}/2\pi)] =$ $[(0.1\ \mathrm{V}, 0.3\ \mathrm{Hz})$, $(0.1\ \mathrm{V}, -0.3\ \mathrm{Hz})$, $(0.5\ \mathrm{V}, -0.3\ \mathrm{Hz})$, $(0.5\ \mathrm{V}, 0.3\ \mathrm{Hz})$,

$(0.1\ \mathrm{V}, 0.3\ \mathrm{Hz})]$, while the parameters follow the reverse sequence in the CCW encircling path. As shown in **Fig. R5**, the results indicate that the system evolves smoothly along the Riemann surface associated with real eigenvalues, exhibiting stable dynamical behavior.

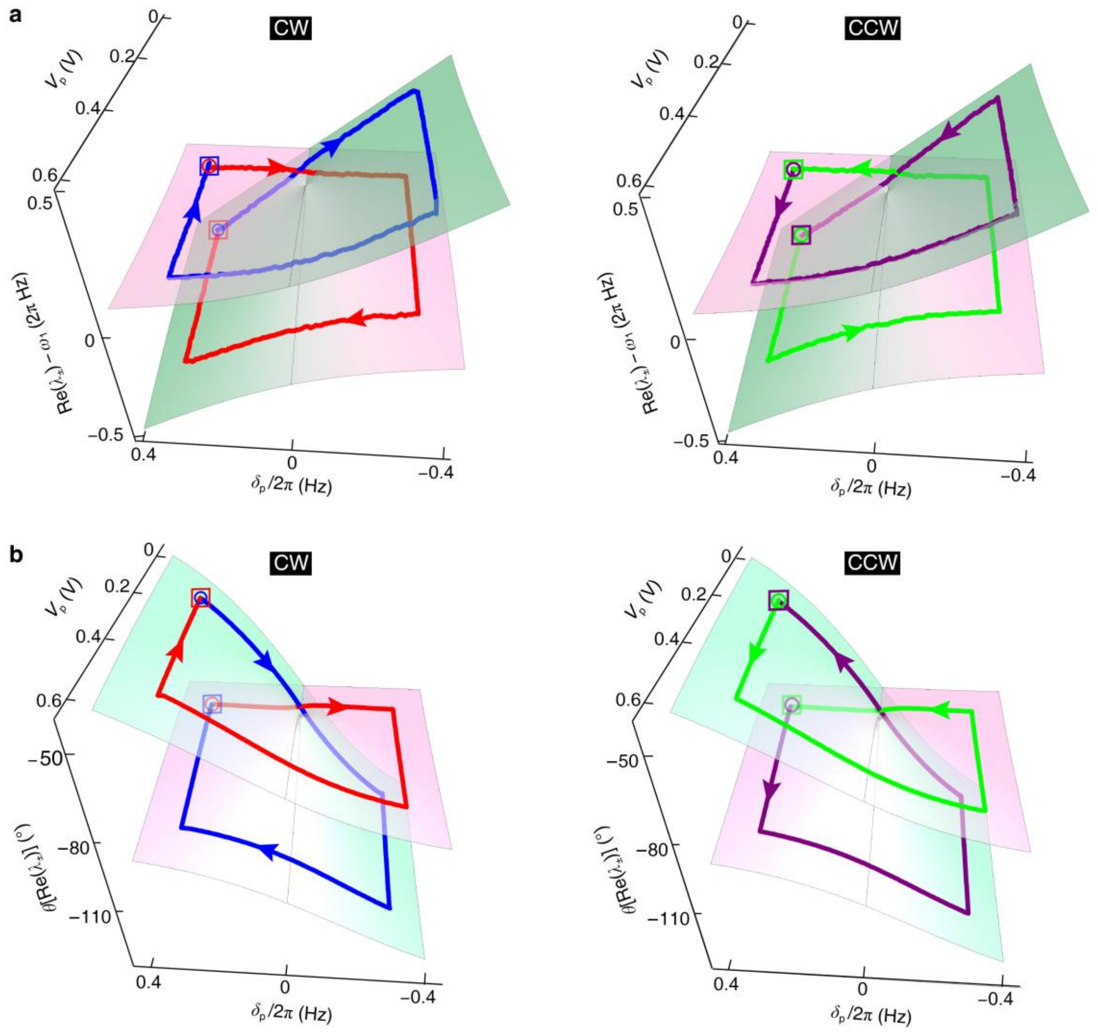

Fig. R5. Results of smooth encircling starting from PT-broken phase obtained using the adaptive phase-tracking technique. a, The phase-tracked closed-loop oscillation frequencies for the CW encircling process starting from the high-frequency sheet (red curve), the CW encircling process from the low-frequency sheet (blue curve), the CCW encircling process from the high-frequency sheet (purple curve), and the CCW encircling process from the low-frequency sheet (green curve) smoothly evolve on the $\mathrm{Re}[\lambda_\pm(t)]$ Riemann surface. The circles and squares denote the start/end points of the encircling trajectories on the high and low-frequency sheets, respectively. The arrow indicates the direction. **b**, The corresponding tracked phases for the four encircling processes. The colors on all the surfaces correspond to the imaginary part $\mathrm{Im}(\lambda_\pm)$ of the eigenvalues.

To summarize, our proposed method for dynamically encircling exceptional points exhibits robustness regardless of the starting point of the encircling.

Changes made:

(1) From Line 19 to Line 21 of Page 9 in the revised manuscript, we have added a clarification as "The base point for the topological encircling is selected as $(\mathrm{V_p}, \delta_\mathrm{p}/2\pi) = (0.5\ \mathrm{V}, 0.3\ \mathrm{Hz})$, which is located in the PT-symmetric phase."

(2) In the revised Section "**Smooth encircling of EP** ", we have added a demonstration about the feasibility of the proposed smooth dynamically encircling when the starting point is in the PT-broken phase:

"To demonstrate that the encircling of EP is not only independent of the encircling direction, but also independent of the position of the starting point, we also conducted an encircling path starting at the PT-broken phase. The base point for the encircling is selected as $(\mathrm{V_p}, \delta_\mathrm{p}/2\pi) = (0.1\ \mathrm{V}, 0.3\ \mathrm{Hz})$, which is located in the PT-broken phase. In the CW encircling path, the control parameters vary linearly by the sequence: $[(\mathrm{V_p}, \delta_\mathrm{p}/2\pi)] = [(0.1\ \mathrm{V}, 0.3\ \mathrm{Hz})$, $(0.1\ \mathrm{V}, -0.3\ \mathrm{Hz})$, $(0.5\ \mathrm{V}, -0.3\ \mathrm{Hz})$, $(0.5\ \mathrm{V}, 0.3\ \mathrm{Hz})$, $(0.1\ \mathrm{V}, 0.3\ \mathrm{Hz})]$, while the parameters follow the reverse sequence in the CCW encircling path. The results of the encircling processes are shown in Fig. 5. The dynamical encircling of EP initiated from the PT-broken phase does not manifest chiral behavior, which demonstrates that the phase-tracked dynamic encircling of the EP enables adiabatic and continuous dynamical evolution."

And Fig. R5 has been included in the revised manuscript "Fig. 5. Results of smooth encircling starting from PT-broken phase obtained using the adaptive phase-tracking technique."

2) The manuscript focuses on the dynamical encircling of a single EP using the PLL-based approach. However, if the system contains two nearby EPs, how does the method extend to characterize or encircle both? Specifically, can the authors shed some light on: How does the PLL technique respond when the control loop passes near or around

both EPs? Does the proximity of the two EPs influence the transport behavior—particularly the emergence or suppression of non-chiral dynamics when the system starts in the symmetry-broken phase? If the control loop encloses both EPs, does the resulting behavior depend solely on the starting point of the loop, or are there qualitatively new phenomena (e.g., interference between EPs or modified topology) that arise?

Response:

We thank the Referee for this constructive suggestion. The question proposed by the Referee is very important for our ongoing future work, and we are now carrying out research on multiple EPs encircling.

In our next work, we construct two nearby EPs in another frequency-matched device using the ordinary stiffness coupling, as seen in **Fig. R4**. In the ordinary coherently coupled non-Hermitian system, the degeneracy and coupling strength of the system are controlled by two DC voltages V_f and V_a, respectively. The two nearby EPs are located at $(V_a, V_f) = (0.8\ \text{V}, 0\ V)$ and $(V_a, V_f) = (-0.8\ \text{V}, 0\ V)$, respectively. Employing this system as a platform, we have conducted two sets of experiments, with the control parameters varying by the sequence of [$(V_a, V_f) = (2.6\ \text{V}, -1.2\ \text{V})$, $(2.6\ \text{V}, 1.2\ \text{V})$, $(-2.6\ \text{V}, 1.2\ \text{V})$, $(-2.6\ \text{V}, -1.2\ \text{V})$, $(2.6\ \text{V}, -1.2\ \text{V})$] and [$(V_a, V_f) =$ $(2.6\ \text{V}, -1.2\ V), (2.6\ \text{V}, 1.2\ V), (0.5\ \text{V}, 1.2\ V), (0.5\ \text{V}, -1.2\ V), (-2.6\ \text{V}, -1.2\ V),$ $(-2.6\ \text{V}, 1.2\ V), (0.5\ \text{V}, 1.2\ V), (0.5\ \text{V}, -1.2\ V),$ $(2.6\ \text{V}, -1.2\ V)$], respectively, which encloses both exceptional points. By using the PLL to lock the phase response to the resonant phase mapped by the eigenfrequency, we can achieve continuous dynamically encircling along Riemann surfaces. As shown in **Fig. R6**, the results demonstrate that non-adiabatic transitions are rigorously excluded during the dynamically encircling process.

Additionally, the dynamically encircling we proposed is **independent of the starting point**. The interaction between the two EPs may involve more profound physical phenomena, and this is also the focus of our next work. We will further report the related results in a follow-up work.

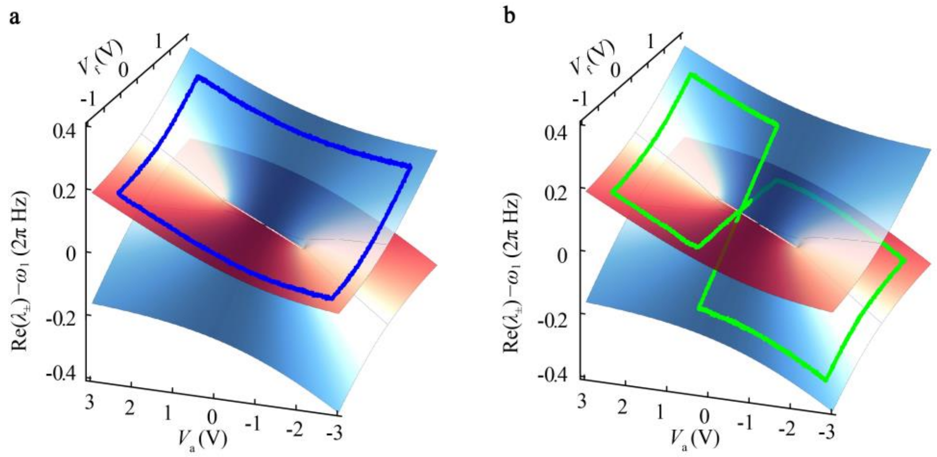

Fig. R6. Results of encircling two EPs through phase-tracked closed-loop control. a, A rectangle loop on the upper sheet of the Riemann surface. **b**, A "∞" trajectory connecting the top-left and bottom-right sheets. All encircling trajectories smoothly evolve along the Riemann surface.

3) How do your findings relate to recent developments in non-Hermitian topology? Specifically, is the phase-tracked dynamical encircling connected to any topological invariants—such as spectral winding numbers—defined over the control parameter loop? Clarifying this connection would help in the broader context of non-Hermitian topological physics.

Response:

We sincerely appreciate your interest in the application of our proposed dynamically encircling method for non-Hermitian topological properties, as well as your invaluable comments and suggestions.

In the **Discussion** section of the main text, we have mentioned that the state of the phase-tracked dynamically encircling can be represented by the hybrid state described by:

$$|\psi\rangle = \frac{-1}{(\lambda_+ - \omega_\mathrm{d})(\lambda_- - \omega_\mathrm{d})}\left(\omega_\mathrm{d} - \Omega_2 + i\frac{\gamma_2}{2}, g\right)^\mathrm{T}$$

where $\lambda_\pm$ corresponds to the system's eigenvalues, and $\omega_\mathrm{d} = \mathrm{Re}[\lambda_\pm]$ represents the real part of $\lambda_{\pm}$, which serves as the resonant frequency of the resonator. By testing the amplitude, phase, and resonant frequency of the dynamically encircling system, we can construct its instantaneous Hamiltonian **H** and reconstruct the imaginary part of the eigenvalues $\mathrm{Im}[\lambda_{\pm}]$, thereby achieving genuine continuous braiding. In this direction, we have made some progress, using the frequency-matched device, we successfully measured the amplitude, phase information of both modes and realized a genuine eigenvalue braiding, as shown in **Fig. R7**.

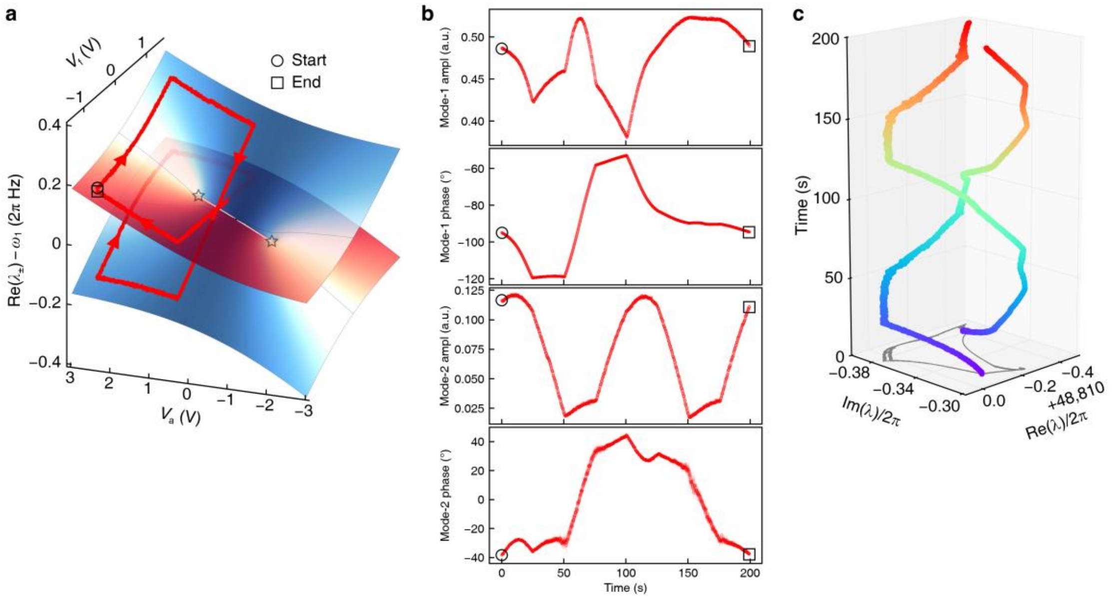

Fig. R7. Genuine braiding of the eigenvalues through dynamically encircling. a, Dynamical encircling path. **b**, Measured amplitude, phase information of both modes. **c**, Reconstructed eigenvalue braiding.

Furthermore, we can reconstruct the instantaneous eigenstates $|v_{\pm}\rangle$ after obtaining the instantaneous eigenvalues $\lambda_{\pm}$ as:

$$|v_{\pm}\rangle = e^{i\alpha}\left(\lambda_{\pm} - \Omega_2 + i\frac{\gamma_2}{2}, g\right)^{\mathrm{T}}$$

where α is an arbitrary phase factor. Based on these theories, we can further investigate the real-time accumulation of the Berry phase in eigenstates. Those results are direct extensions of this work and will be presented in our forthcoming work.

Response to Reviewers

Please find below our response to the reviewers. Reviewers' comments are in **blue**, and authors' responses are in **black**.

Reviewer #1 (Remarks to the Author):

The authors have addressed all my concerns in a satisfactory way. I sincerely thank the authors for their efforts in improving their work. I recommend the publication of the work in its present form.

Response:

Thank you very much for your valuable and constructive comments. The feedback has greatly enhanced our manuscript.

Reviewer #2 (Remarks to the Author):

The authors have made significant efforts in improving the manuscript. The revised manuscript can be accepted as is now.

Response:

We would like to express our sincere thanks to you for the valuable feedback, which is very constructive for revising the manuscript.

Reviewer #3 (Remarks to the Author):

The authors have thoroughly addressed the previous concerns, and the refined version of the manuscript significantly improves the overall quality, clarity, and impact of the work. The revisions strengthen the presentation and resolve the issues raised in the earlier review. I find that the manuscript now meets the standards required for publication and can be recommended for publication in its current form.

Response:

Thank you very much for your constructive comments and suggestions, which not only improved our paper but also inspired our future work.